J. Chem. Sci. Vol. 127, No. 12, December 2015, pp. 2183–2191.
DOI 10.1007/s12039-015-0968-x

Radical Scavenging Efficacy of Thiol Capped Silver Nanoparticles

KUMUDINI CHANDRAKER[a], SANDEEP KUMAR VAISHANAV[a], REKHA NAGWANSHI[b] and MANMOHAN L SATNAMI[a,*]

[a]School of Studies in Chemistry, Pt. Ravishankar Shukla University, Raipur 492 010, India
[b]Department of Chemistry, Govt. Madhav Science P. G. College, Ujjain (M.P.), 456 010 India
e-mail: manmohanchem@gmail.com

MS received 10 July 2015; revised 26 August 2015; accepted 11 September 2015

Abstract. Radical scavenging efficacy of L-cysteine (L-Cys), glutathione (GSH) and thioctic acid (TA) in the presence of silver nanoparticles (AgNPs) were determined by 1,1-diphenyl 2-picryl hydrazil (DPPH), nitric oxide (NO) and hydroxyl (OH) radicals as spectrophotometric assay. The hydrogen peroxide (H_2O_2) scavenging efficacy has been determined by titration method. Ascorbic acid has been used as standard for all radical scavenging efficacies. In general, antioxidant activity decreases in the presence of AgNPs. The covalent interactions of thiols (-SH) were found to be a key factor for the decreases in scavenging activity. The effect of thiol concentrations has been discussed. The size and shape of the nanoparticles and AgNP-SR interactions have been characterized through Transmission Electron Microscopy (TEM) and Fourier Transform Infrared (FTIR) spectroscopy, respectively.

Keywords. Silver nanoparticle; radical scavenging efficacy; Thiol; DPPH.

1. Introduction

Radical scavengers (RS) are highly reactive species that can potentially abstract hydrogen atoms from activated bonds of biological materials under physiological environment. RS plays crucial role in neutralizing the direct attack of reactive oxygen species (ROS) that prevents anumber of acute and chronic cellular implications by inhibiting the oxidative damage.[1] Thiolated antioxidants such as L-cysteine (L-Cys), glutathione (GSH) and dihydrolipoic acid (DHLA) provide important physiological defense against oxidative damage, which are derived from natural rather than synthetic source.[2] L-Cys is an important thiol in living organisms, an active center in protein as well as in the tripeptide GSH, plays a vital role in the reversible redox reactions in cells to limit cellular damage attributable to ROS.[3] GSH has various physiological functions, such as detoxification, preservation of crucial thiol status, antioxidant activity, and regulation of growth and death.[4] 1,1-diphenyl 2-picryl hydrazil (DPPH) is a stable and well characterized synthetic solid radical for estimation of scavenging activity of compounds.[5,6] Nitric oxide (NO) radical is avery labile species which is involved in many biological functions like inhibition of platelet aggregation,[7] neurotransmission[8] and cell mediated immune responses.[9,10] The strong oxidizing nature of hydroxyl (OH) radical generated inside the cells can cause irreparable cellular damage to cellular proteins, lipids and DNA.[11–14] A simple schematic reaction mechanisms of radical scavenging process of thiolated antioxidants via DPPH, NO and OH free radicals are shown in (scheme 1).

Metal nanoparticles, such as silver and gold are the most familiar metal based nanoparticles used for medicinal applications which can be traced back for centuries. Current nanotechnology facilitates more extensive and sophisticated applications of nanosilver in foods, health care and consumer products as antimicrobial agents.[15–19] A large number of researchers have studied the cytotoxicity and genotoxicity due to exposure of silver nanoparticles (AgNPs).[20] The bioactivity and potential toxicity of AgNPs can be well understood by considering their interactions with the components of biological systems. The intensive studies on the participation of AgNPs in redox reactions, lead to understand the effect of AgNPs on cellular components involved in redox homeostasis. Nature of bonding of thiols on the AgNP surface has important physical and chemical properties and has led to many profitable applications. The interaction between AgNPs and sulfur atoms are satisfactorily strong to allow immobilization of thiolated species.[21–23] AgNPs have ability of surface functionalization by the action with compounds bearing a thiol (-SH) or disulfide (RS-SR) moiety.[24–28]

*For correspondence

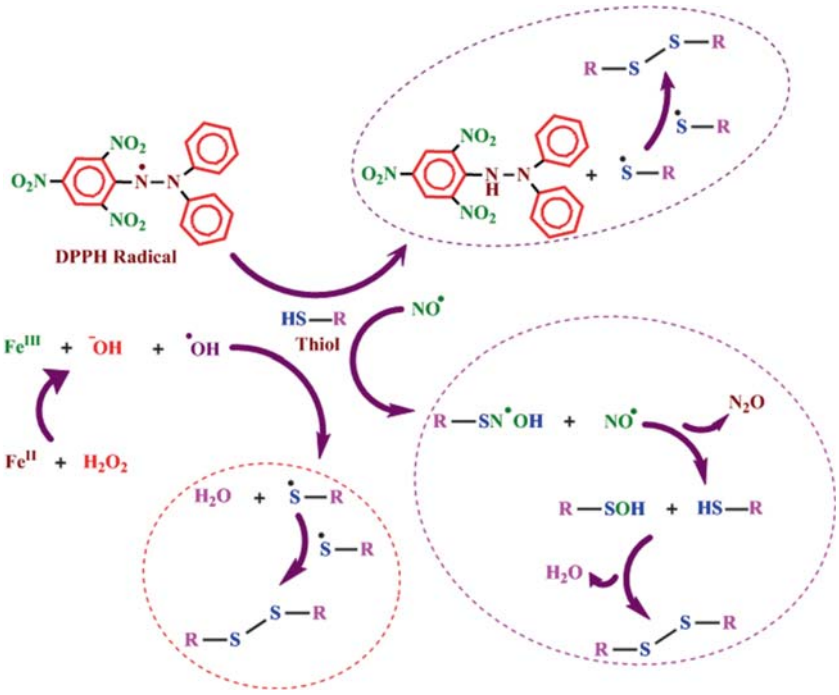

Scheme 1. Hydrogen abstraction of thiol by DPPH, NO and OH radical scavengers.

The new nanomaterial-based method for estimating the antioxidant activity relies on the thiol protected AgNPs and optical monitoring of the corresponding plasmon absorption bands. The antioxidant properties of thiol ligands such as thioctic acid (TA), L-Cys and GSH (chart 1) have been extensively investigated. In the present paper, an attempt has been made to investigate the effects of thiolated ligand on the stability of AgNPs and kinetics of DPPH radical scavenging efficacy of all three thiolated ligand in presence of AgNPs. The radical scavenging assay provides an alternative perspective of nanoparticles for the estimation of DPPH, NO, OH radicals and hydrogen peroxide (H_2O_2) scavenging ability. Comparative studies of the radical scavenging behavior of thiolated antioxidants (alone) and in presence of AgNPs have been discussed.

2. Experimental

2.1 *Materials and Methods*

Silver nitrate ($AgNO_3$, 99%), trisodium citrate dihydrate ($HOC(COONa)(CH_2COONa).2H_2O$), sodium borohydride ($NaBH_4$), thioglycolic acid (TGA) ($HSCH_2COOH$, 98%), L-cysteine hydrochloride monohydrate (98%), thioctic acid ($HSC_7H_{12}2COOH$, 98%), glutathione (reduced) and ascorbic Acid ($C_6H_8O_6$) were purchased from Sigma Aldrich. Purified water with a Millipore Mili-Q-water system was used.

2.2 *Synthesis of Silver Nanoparticles*

All glasswares used in the preparation of AgNPs were cleaned with aqua regia (3:1HCl/HNO_3), rinsed with

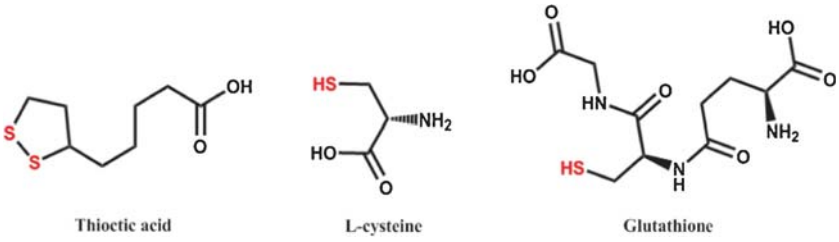

Chart 1. Chemical structure of thioctic acid, L-cysteine and glutathione.

distilled water and dried. Citrate functionalized silver nanoparticles (CF-AgNPs) were synthesized by Martins method.[26] Briefly, 0.25 mM trisodium citrate was added to 100 mL aqueous solution of $AgNO_3$ (0.25 mM) with continuous stirring and followed by adding freshly prepared 0.1 M aqueous sodium borohydride, dropwise for desired concentration. Upon addition of $NaBH_4$, the color of the solution turned yellow, which indicates the formation of AgNPs. The resulting AgNPs has a diameter of 5.0 ± 1.2 nm resolved by TEM.

2.3 *Synthesis of Thiol Capped Silver Nanoparticles*

CF-AgNPs stabilized by the addition of TA (0.25–1.0 mM ethanolic solution) to AgNPs solution (0.23 nM) and the pH was readjusted to 11.67 using dilute NaOH. For complete stabilization and ligand exchange, the above prepared reaction solution was kept at least 18 h in dark with continuous stirring. Similarly, L-Cys and GSH capped AgNPs (i.e. L-Cys@AgNPs and GSH@AgNPs) have been prepared by adding 0.25 to 1.0 mM of L-Cys and GSH to the AgNPs solution (0.23 nM) under continuous stirring, respectively.

2.4 *UV-visible Spectroscopic Analysis*

The plasmon resonance of AgNPs and its antioxidant activity were studied with Thermo scientific evolution-300 UV-visible spectrophotometer.

2.5 *Fourier Transform Infrared (FTIR) Spectroscopic Analysis*

The FTIR spectral scans of pure TA, L-Cys and GSH and their corresponding AgNPs in the region 4000–400 cm^{-1} were recorded by employing Fourier transform infrared spectrometer (DRS–FTIR) equipped with deuterated, L–alanine doped triglycine sulfate (DLaTGS) detector (Model: Nicolet iS10, Thermo fisher Scientific Instrument, Madison, USA).

2.6 *Transmission Electron Microscopy (TEM)*

The morphology and diameter of the AgNPs were characterized on a JEOL, JEM-2100F Transmission Electron Microscopy (TEM) using an acceleration voltage of 200 kV. The samples were prepared by taking a few drops of AgNPs solution on a carbon film covered with copper grid. Excess NPs from the test solution were detached by filter paper before drying the sample. The resulting images were analyzed through image pro analyzer.

2.7 *In vitro antioxidant Assays*

2.7a *1,1-diphenyl 2-picryl hydrazil (DPPH) radical scavenging assay*: The scavenging activity against DPPH free radical was designed according to Zhao *et al*.[29] The antioxidant property of thiol and AgNPs have been evaluated by monitoring their quenching capacity against synthetically stable DPPH radical. The solution containing 1.5 mL of different concentrations of thiol (0.25–1.0 mM) capped AgNPs were added to 1.5 mL of 0.25 mM DPPH. These solution mixtures were incubated for 30 min at 37°C and the change in color was observed spectrophotometrically at 517 nm. Equation (1) was used for the determination of the radical-scavenging activity (RSA):

$$\%\,\mathrm{RSA} = \left[\frac{A_{\mathrm{DPPH}} - A_S}{A_{DPPH}}\right] \tag{1}$$

Where, A_S is absorbance of DPPH solution with nanoparticles and A_{DPPH} is absorbance of DPPH solution without nanoparticles.[30] Ascorbic acid was used as standard antioxidant agent.

2.7b *Nitric oxide radical scavenging assay*: NO radical scavenging assay was designed according to Kang et al.[31] NO radical scavenging properties of thiol capped AgNPs were evaluated by NO radical scavenging assay. NO assay was performed by mixing 1.0 mL of 5.0 mM sodium nitroprusside with 1.0 mL of different concentration of thiol (0.25–1.0 mM) capped AgNPs. The mixtures were incubated for 60 min at room temperature. After incubation, an equal amount of Griess reagent (1% sulphanilamide, 2% phosphoric acid, and 0.1% napthylethylene diamine dihydrochloride) was added to the reaction mixture and absorbance was measured at 546 nm. Ascorbic acid was used as a standard antioxidant agent.

2.7c *Hydroxyl radical scavenging assay*: OH scavenging activity of AgNPs was measured according to Yu *et al.*[32] Reaction mixture containing 60 μL of 1.0 mM $FeCl_2$, 90 μL of 1 mM 1,10-phenanthroline, 2.4 mL of 0.2 M phosphate buffer (pH 7.8), 150 μL of 0.17 M H_2O_2, and 1.5 mL of different concentration of thiol (0.25–1.0 mM) capped AgNPs were incubated at room temperature for 5 minutes. After incubation, scavenging activity of the AgNPs was measured spectrophotometrically and evaluated against the standard ascorbic acid by equation 1.

2.7d *Hydrogen peroxide scavenging assay*: H_2O_2 scavenging activity of nanoparticles was evaluated by replacement titration according to Zhao et al.[29] A 1.0 mL of 0.1 mM H_2O_2 was mixed with 1.0 mL of different concentration of thiol (0.25–1.0 mM) capped AgNPs, followed by addition of 2 drops of 3% ammonium molybdate, 10 mL of 2 M H_2SO_4 and 7.0 mL of 1.8 M KI. The reaction mixture was titrated with 5.09 mM $Na_2S_2O_3$ until the disappearance of yellow color.

3. Results and Discussion

3.1 *Characterization of TA@AgNPs, L-Cys@AgNPs and GSH@AgNPs*

Surface capping agent plays a very important role in controlling the size and morphology of the nanostructures. Ionic surface stabilizing agent adsorbs onto the nanoparticle surface and generates a uniform charge on the particle surface. It is therefore possible to generate very stable and uniform sized nanoparticles by reducing the agglomeration tendency of the particles.[31] The plasmonic absorption bands of the metal nanoparticles were used for characterization of the nanoparticles. AgNPs exhibit a characteristic surface plasmon resonance (SPR) band at 400 nm. The effects of different ligands on SPR band of AgNPs are shown in figure 1. The effect of initial concentration of $AgNO_3$ on TA@AgNPs infers that very sharp and intense band was observed at higher concentration and suggested the linear relationship between intensity of band and initial concentration of $AgNO_3$ (figure S1a, see Supplementary Information). TA provides improved stabilization by Ag-S covalent interaction, which is significantly reflected in its SPR band intensity. This behavior might be due to cross linking, which was marked at lower concentrations of $AgNO_3$ as compared to TA. The pH dependent optical behavior of TA@AgNPs demonstrates that most of the ions are present in its (COO- as well as –S-) ionic state at pH greater than pK_a which result in electrostatic stabilization of AgNPs, that is more pronounced at higher pH (figure S1 b). At higher pH of 11.67 the disulfide bond of TA breaks, hence two free –S groups were produced per TA molecule which is capping AgNPs by covalent interaction between S-Ag.[33] Concentration dependent representative sets of the SPR band of TA@AgNPs (figure 1A) shows that the intensity of SPR band was found to be inversely proportional to the concentration of TA, which suggests that the decrease in SPR band intensity without any shift might be due to the cross-linking between the adjacent active functional groups present on the AgNPs surface. The shift towards longer wavelength can be attributed to the cross-linking phenomenon that was more pronounced at higher concentration. Similar results were also observed for L-Cys@AgNPs and GSH@AgNPs (figure 1, B and C). These spectral changes indicate that the AgNPs were aggregating and may be attributed to the formation of Ag−S bond and cross-linking between the adjacent groups.

The interactions of TA, L-Cys and GSH with AgNPs have been studied through FTIR spectral analysis. The FTIR spectra of pure TA and TA@AgNPs recorded in a spectral window from 400 to 4000 cm^{-1} are shown in figure 2A. The bands at 2931 cm^{-1} and 735 cm^{-1} correspond to the –C-H and weak S-S stretching vibrations, respectively, but this weak S-S band is absent in TA@AgNPs. These spectral changes can be attributed to the deprotonation and formation of Ag–S. Similar spectral changes were also observed for pure L-Cys, GSH and their corresponding AgNPs (figures 2B and 2C), where ν (-SH) appeared at 2560 cm^{-1} and 2524 cm^{-1} for L-Cys and GSH, respectively, that disappeared in their corresponding stabilized AgNPs. These

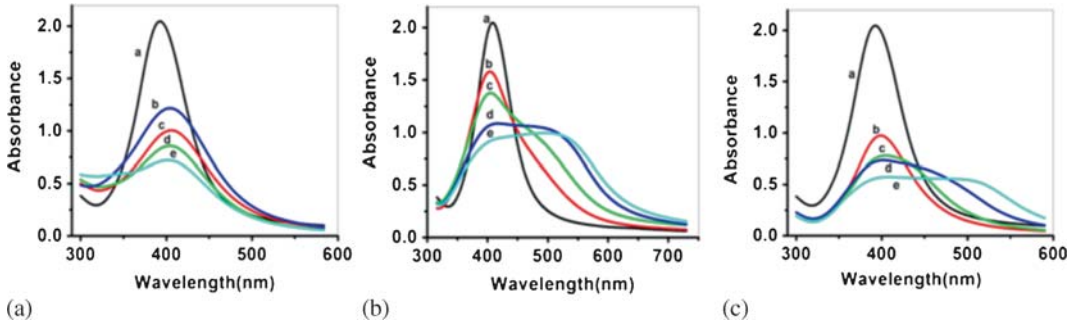

Figure 1. Effect of ligand concentration on AgNPs. (A) Effect of TA (mM): (a) 0.00, (b) 0.25, (c) 0.50, (d) 0.75 and (e) 1.0 mM. (B) Effect of L-Cys (mM): (a) 0.00, (b) 0.25, (c) 0.50, (d) 0.75, (e) 1.0 mM. (C) Effect of GSH (mM): (a) 0.00, (b) 0.25, (c) 0.50, (d) 0.75, (e) 1.0 mM.

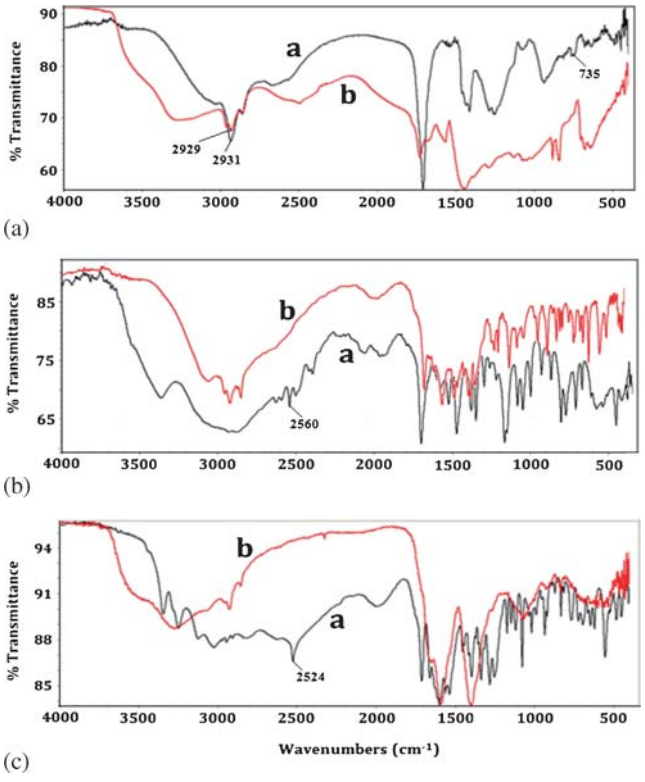

Figure 2. FTIR spectra of thiol and AgNPs (A) TA (a) and TA@AgNPs (b); (B) L-Cys (a), L-Cys@AgNPs (b); and (C) GSH (a), GSH@AgNPs (b).

significant changes in the FTIR spectra, especially in S-H stretching bands suggested the fruitful interaction of ligands with AgNPs surface.

The size and morphology of AgNPs are shown in figure 3. TEM image of CF-AgNPs (figure 3A) displayed particles with average size of 5.0 ± 1.2 nm. It indicates that most of the particles are spherical shaped with uniform size, which is also supported by the histogram. High-resolution Transmission Electron Microscopic (HRTEM) image and Selected Area Electron Diffraction (SAED) pattern provide information about the phase structure and crystal symmetry of AgNPs. The interplanar distance was found to be 0.255 nm that suggests the face centered cubic (FCC) structure for CF-AgNPs. Similarly, figure 3B shows TEM image of TA@AgNPs (optimum concentration of TA 0.50 mM), their corresponding HRTEM image and SAED pattern. TEM images of TA@AgNPs displayed monodispersity with average particle size of 5.0 ± 0.1 nm which is well supported by the histogram. Figure 3B (a) indicates that nanoparticles are well separated from adjacent nanoparticles, which illustrates that surface of AgNPs is well stabilized by TA molecules at pH value ~11.67. SAED pattern and HRTEM images suggest that TA@AgNPs have similar crystal structure as CF-AgNPs with interplanar distance (d) of 0.267 nm. GSH is bigger ligand than L-Cys, and L-Cys@AgNPs showed faster aggregation as compared to GSH@AgNPs. Figure 3 (C & D) illustrates the TEM images of L-Cys@AgNPs and GSH@AgNPs prepared at 0.25 mM concentration of L-Cys and GSH, respectively. The size of the nanoparticles depends on the concentration of thiolated ligand. At higher concentrations, particles overlap with

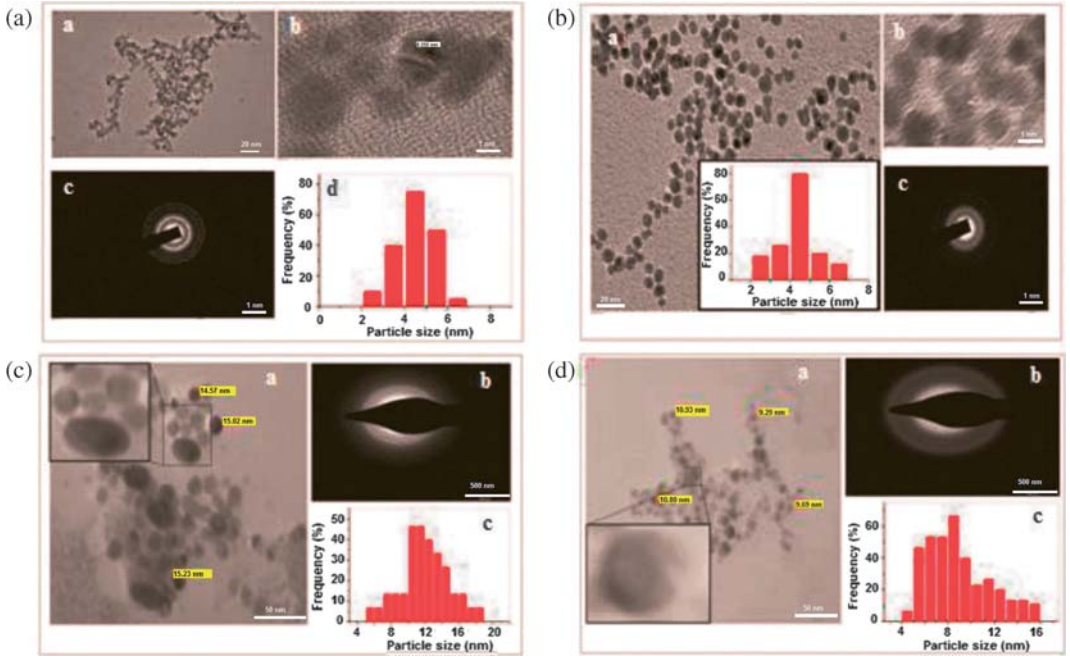

Figure 3. TEM image, HRTEM image, SAED pattern and histogram of particle size distribution of (A) CF-AgNPs, (B) TA@AgNPs, (C) L-Cys@AgNPs and (D) GSH@AgNPs.

their adjacent active functional groups and are flocked, which result in larger or rod shaped AgNPs. The larger size AgNPs compared to TA@AgNPs can be seen in Figure 3 (C & D). The average particle size is found to be 15.4 ± 0.7 nm and 11.6 ± 1.4 nm for L-Cys@AgNPs and GSH@AgNPs, respectively. The increased size can be attributed to the aggregation of AgNPs by L-Cys and GSH.[34] The histograms for L-Cys@AgNPs and GSH@AgNPs indicate the non-uniform size distributions of AgNPs.

3.2 *Antioxidant Study*

AgNPs and thiol capped AgNPs have numerous applications, e.g., antioxidant activity, it depends on the inhibition of oxidation of molecule by inhibiting the initiation step of oxidative chain reactions and formation of stable free radicals. Free radicals are unstable and they tend to form stable bond, by accepting or donating the electrons to quench radical. The DPPH is a stable, nitrogen centered free radical which has a

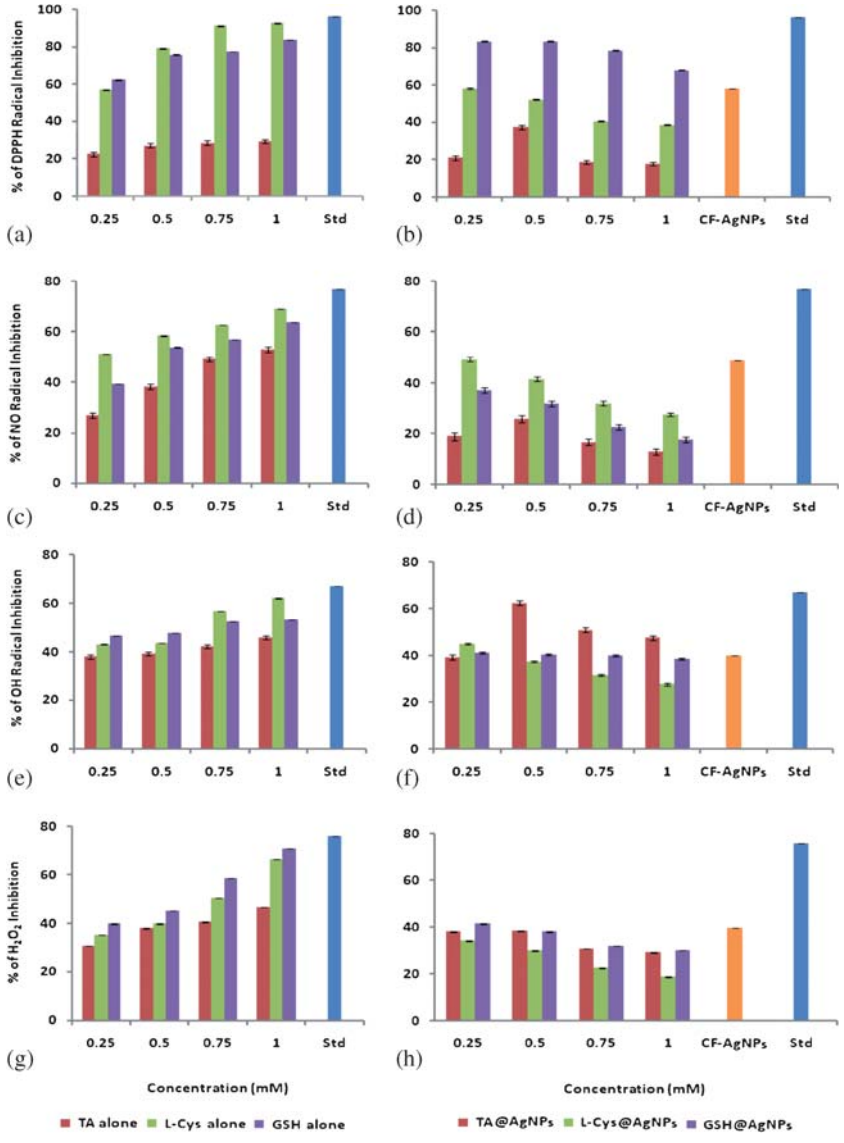

Figure 4. Radical scavenging by antioxidants: (a) DPPH (b) NO (c) OH (d) H_2O_2, activity upon thiolated ligands and their corresponding AgNPs. (e) DPPH radical scavenging activity of TA@AgNPs, L-Cys@AgNPs and GSH@AgNPs; (f) NO radical scavenging activity of TA@AgNPs, L-Cys@AgNPs and GSH@AgNPs; (g) OH radical scavenging activity of TA@AgNPs, L-Cys@AgNPs and GSH@AgNPs; and (h) H_2O_2 scavenging activity of TA@AgNPs, L-Cys@AgNPs and GSH@AgNPs. Ascorbic acid was used as standard.

very strong absorption band at 517 nm. The antioxidant activity of any species can be determined spectrophotometrically by monitoring the change in color of DPPH from violet to yellow. The change in color is attributed to the reduction of DPPH either by hydrogen or electron donation. The percentage inhibition of DPPH radical is presented in figure 4(a and e). It represents the DPPH radical scavenging activity profile of free thiolated antioxidants (TA, L-Cys and GSH) and thiolated ligand that are covalently bound to AgNPs. It infers that the DPPH radical scavenging activity of TA, L-Cys and GSH increases with increasing the concentration of thiolated agent. Moreover, in the case of L-Cys@AgNPs and TA@AgNPs, the DPPH radical scavenging activity was significantly lowered as compared to its free state. Gradual decrease in radical scavenging activity was observed for L-Cys@AgNPs while in the case of TA@AgNPs, the scavenging activity reached maxima at 0.50 mM concentration and forms more stable AgNPs and then it gradually decreases with increasing the concentration of TA (0.75 mM to 1.0 mM). However, different results were observed in case of GSH@AgNPs; DPPH scavenging activity was found to be decrease with increasing concentration of GSH (0.25 mM to 1.0 mM). These results are consistent with the UV-visible spectra where high concentration of thiolated ligand leads to the agglomeration of AgNPs which in turn lowers DPPH radical scavenging property of thiol stabilized AgNPs. CF-AgNPs show better radical scavenging activity (58.49%) of DPPH compared to TA@AgNPs and L-Cys@AgNPs, which might be because Ag shows good antioxidant property and can easily lose electrons. However, GSH@AgNPs established greater antioxidant capacity than CF-AgNPs. The DPPH radical scavenging activities were examined against ascorbic acid (96.34%) as standard.

The DPPH radical scavenging efficacy of thiol capped AgNPs was monitored with time using UV-visible spectrophotometer. The % DPPH inhibiton of thiol capped AgNPs were monotonically increasing with time (figure 5). The % inhibition depends on the interaction between thiolated ligand and AgNPs, which directly depends on the structure of ligands. TA@AgNPs shows minimal % inhibition while GSH@AgNPs shows maximum % inhibition that can be explained on the basis of their structures. TA have two free –SH in its reduced form and therefore it shows greater interaction with AgNPs, while GSH has only one –SH group per molecule. Hence, despite of being a very good stabilizing agent it shows less interaction with AgNPs compared to TA which reflects in its % inhibition property. The % inhibition of L-Cys@AgNPs is intermediate between TA@AgNPs and GSH@AgNPs that is due to its strong interaction with AgNPs respective to its smaller size.

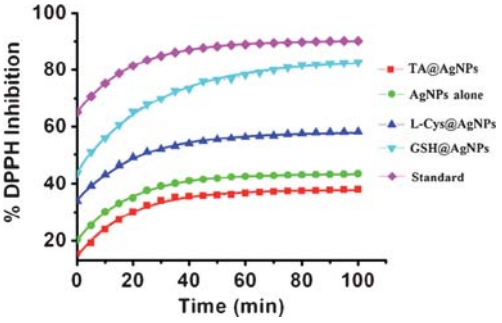

Figure 5. Time dependence of % DPPH inhibition of different thiol (0.25 mM) capped AgNPs against standard ascorbic acid.

NO radical scavenging capacity of any species can be determined by using Griess reagent, which forms a colored complex formazone that can be measured spectrophotometrically. NO radical is a highly reactive species that can be reduced by accepting electrons from thiolated ligand, AgNPs and thiol protected AgNPs. The percentage inhibition of NO radical is presented in figure 4 (b and f). Similar behavior like DPPH assay was observed in the NO radical inhibition activity of TA, L-Cys and GSH. Results indicate that the percentage inhibition of NO radical increases with increasing the concentrations of thiolated antioxidants. Comparable results as free ligands were observed in case of TA@AgNPs where concentration is directly proportional to the inhibition activity against NO radical (table S2, see Supplementary Information). But a marked reduction in inhibition activity was observed compared to free TA, which might be due to the incorporation of thiol groups in stabilization of AgNPs which in turn lowered the electron releasing capacity of TA. However, GSH@AgNPs displayed just the reverse behavior as that of free GSH. The percentage inhibition of GSH@AgNPs (17.76%) (table S2) was considerably less compared to free GSH (63.87%) (table S1). L-Cys@AgNPs shows quite a different behavior as compared to other AgNPs. The inhibitory activity of L-Cys@AgNPs was found to be maximum at 0.50 mM and then a gradual decrease was observed. These results indicate that at higher concentration, L-Cys@AgNPs and GSH@AgNPs clumped with each other through cross-linking. The cross linking makes active functional group entangled to each other. This phenomenon is responsible for marked reduction in inhibition activity of thiol stabilized AgNPs. CF-AgNP shows 49.01% of NO radical scavenging activity. All the NO radical scavenging activity

were compared against ascorbic acid (76.97%) as standard.

OH radicals originated from FENTON reaction was used as a tool to determine the radical scavenging activity of free thiolated antioxidants and their corresponding thiol stabilized AgNPs (figure 4c and g). The OH radical scavenging activity of TA, L-Cys and GSH in its free state and its corresponding bound state to AgNPs have been investigated. Similar radical scavenging activity profile like DPPH assay has been observed in free thiolated antioxidant (TA, L-Cys, and GSH) and thiolated ligand that are covalently bound to AgNPs. TA shows better OH radical scavenging activity 46.03% (table S1) as compared to DPPH radical inhibition activity 29.35% (table S1), while just reverse scenario has been observed in the case of L-Cys and GHS (table S1). It is inferred that the OH radical scavenging activity of L-Cys, GSH and TA increases with increasing the concentration of thiolated agent that can be attributed to the increased concentration of thiol (–SH) groups. However, in L-Cys@AgNPs and GSH@AgNPs, the OH radical scavenging activity was found to be inversely proportional to the concentration of thiol under the optimized condition. L-Cys@AgNPs and GSH@AgNPs show maximum inhibition percentage 45.16% and 41.20%, respectively, at its initial concentration 0.25 mM and then gradually decrease (table S2). In case of TA@AgNPs the percentage inhibition of OH radical attained its maximum (62.58%) at 0.50 mM and then a constant decrease was observed. CF-AgNPs represent (40.10%) OH radical scavenging activity.

H_2O_2 scavenging assay is another very useful assay for evaluating the radical scavenging property of any species. Similar experiments as DPPH assay were carried out with thiolated antioxidant (TA, L-Cys, and GSH) and their corresponding AgNPs (figure 4d and h). Here, in this assay L-Cys and GSH show quite different results as compared to the above three methods. L-Cys shows a maximum percentage inhibition (66.48%) at 1.0 mM (table S1) while in case of GSH, percentage H_2O_2 inhibition was comparatively greater than L-Cys. However, in case of TA the percentage H_2O_2 inhibition was found to be directly proportional to the concentration (table S1). All the results were compared to ascorbic acid (76.02%) as standard. Similarly, the percentage H_2O_2 inhibition was also investigated for corresponding AgNPs. TA@AgNPs showed similar behavior like free L-Cys where it attained its maximum (38.37%) at 0.50 mM (table S2) and then gradually decreased. However, in the case of L-Cys@AgNPs and GSH@AgNPs, the percentage H_2O_2 inhibition was inversely proportional to the concentration of L-Cys and GSH. The maximum percentage inhibition of L-Cys@AgNPs and GSH@AgNPs was calculated to be 34.19% and 41.48%, respectively at 0.25 mM (table S2). The results suggested that the high concentration of L-Cys and GSH, promotes the agglomeration of AgNPs, which causes a marked reduction in the number of electron donating moieties, which in turn results in the lowered inhibition activity. The above results are also supported by UV-visible spectra. The CF-AgNPs showed (39.89%) H_2O_2 inhibition.

4. Conclusions

Radical scavenging efficacy of biologically essential antioxidants (TA, L-Cys and GSH) in its free state and in presence of AgNPs have been investigated through different radical scavenging assay i.e., DPPH, NO, OH and H_2O_2 assay. In the present investigation we found that radical scavenging efficacy of thiolated antioxidants was decreased in presence of AgNPs which is due to the covalent interaction of -SH with AgNPs. Concentration of thiol was found directely proportional to the radical scavenging efficacy for free thiol while in case of thiol-AgNPs, it decreases after attaining a maximum radical scavenging efficacy. Kinetic plot of % DPPH inhibition of thiol-AgNPs inferred that the minimal % DPPH inhibition was observed for TA@AgNPs while maximum inhibition observed for GSH@AgNPs that might be due to the smaller size with two SH group facilitate stronger coordination compared to bulkier GSH molecule with one –SH group. Similarly the smaller size of L-Cys induces faster aggregation among L-Cys@AgNPs that leads to lesser % DPPH inhibition compared to GSH@AgNPs. The ligand size-radical scavenging activity relationship obtained in this study provides valuable and fundamental information about the scavenging behavior of thiol capped AgNPs in biological system.

Supplementary Information

All additional information, namely, effect of concentration of $AgNO_3$ on TA@AgNPs and effect of pH on TA@AgNPs (figure S1) are given in the Supplementary Information. Percentage of DPPH, NO, OH radical inhibitions and H_2O_2 inhibition of TA, L-Cys and GSH with various concentrations (table S1) and percentage of DPPH, NO, OH radical inhibitions and H_2O_2 inhibition of TA@AgNPs, L-Cys@AgNPs and GSH@AgNPs with various concentrations of TA, L-Cys and GSH, respectively (table S2) are also given in

the Supporting Information which is available at www.ias.ac.in/chemsci.

Acknowledgements

Authors are thankful to sophisticated analytical instrument research facility (AIRF) at Jawaharlal Nehru University (JNU), New Delhi for TEM analysis. Authors are thankful to the Head, School of Studies in Chemistry, Pt. Ravishankar Shukla University, Raipur for providing laboratory facilities.

References

1. Havsteen B H 2002 *Pharmacol. Therapeut.* **96** 67
2. Mitchell S C 2003 In *Biological Interaction of Sulfur Compound* S C Mitchell (Ed.) (London: CRC Press) p. 20
3. Wlodek L 2002 *Pol. J. Pharmacol.* **54** 215
4. Lu S C 2009 *Mol. Aspects Med.* **30** 42
5. McGowan J C, Powell T and Raw R 1959 *J. Chem. Soc.* 3103
6. Hogg J S, Lohmann D H and Russell K S 1961 *Can. J. Chem.* **39** 1588
7. Radomski M W, Palmer R M J and Moncada S 1987 *Br. J. Pharmacol.* **92** 181
8. Knowles R G, Palacios M, Palmer R M J and Moncada S 1989 *Proc. Natl. Acad. Sci. USA* **86** 5159
9. Marletta M A, Yoon P S, Iyengar R, Leaf C D and Wishnok J S 1988 *Biochemistry* **27** 8706
10. Hibbs J B, Taintor R R, Vavrin Z and Rachelin E M 1988 *Biochem. Biophys. Res. Commun.* **157** 87
11. Halliwell B and Gutteridge J M C 1992 *FEBS Lett.* **307** 108
12. Stamler J S, Singel D J and Loscalzo J 1992 *Science* **158** 1898
13. Ames B N, Shigenaga M K and Hagen T M 1993 *Proc. Natl. Acad. Sci. USA* **90** 7915
14. Edward G J 1984 *Methods Enzymol.* **105** 188
15. Maillard J Y and Hartemann P 2012 *Crit. Rev. Microbiol. Early Online* 1
16. Geranio L, Heuberger M and Nowack B 2009 *Environ. Sci. Technol.* **43** 8113
17. Wilkinson L J, White R J and Chipman J K 2011 *J. Wound Care* **20** 543
18. Nobile M A D, Cannarsi M, Altieri C, Sinigaglia M, Favia P and Iacoviello G 2004 *J. Food Sci.* **69** 379
19. Benn T M and Westerhoff P 2008 *Environ. Sci. Technol.* **42** 4133
20. de Lima R, Seabra A B and Duran N 2012 *J. Appl. Toxicol.* **32** 867
21. Ulman A 1996 *Chem. Rev.* **96** 1533
22. Rodriguez J A, Dvorak J, Jirsak T, Liu G, Hrbek J, Aray Y and Gonzalez C 2003 *J. Am. Chem. Soc.* **125** 276
23. Roux S, Garcia B, Bridot J L, Salome M, Marquette C, Lemelle L, Gillet P, Blum L, Perriat P and Tillement O 2005 *Langmuir* **21** 2526
24. Chen S and Sommers J M 2001 *J. Phys. Chem. B* **105** 8816
25. Anyaogu K C, Fedorov A V and Neckers D C 2008 *Langmuir* **24** 4340
26. Daniel M C and Astruc D 2004 *Chem. Rev.* **104** 293
27. Brust M and Kiely C J 2002 *Colloids Surf. A* **202** 175
28. Fernandez C A and Wai C M 2006 *Small* **2** 1266
29. Zhao G R, Xiang Z J, Ye T X, Yuan Y J and Guo Z X 2006 *Food Chem.* **99** 767
30. Shimada K, Fujikawa K, Yahara K and Nakamura T 1992 *J. Agri. Food. Chem.* **40** 945
31. Kang K S, Yokozawa T, Kim H Y and Park J H 2006 *J. Agri. Food. Chem.* **54** 2558
32. Yu W, Zhao Y and Shu B 2004 *Food Chem.* **86** 525
33. Lin S Y, Tsai Y T, Chen C C, Lin C M and Chen C H 2004 *J. Phys. Chem. B* **108** 2134
34. Majzik A, Fulop L, Csapo E, Bogar T, Martinek T, Penke B, Biro G and Dekany I 2010 *Colloids Surf. B: Biointerfaces* **81** 235